Universality classes of the θ and θ' points

Peter H. Poole

Department of Physics, Saint Francis Xavier University, Antigonish, Nova Scotia, Canada B2G 1C0
and Center for Polymer Studies and Department of Physics, Boston University, Boston, Massachusetts 02215

Antonio Coniglio

Center for Polymer Studies and Department of Physics, Boston University, Boston, Massachusetts 02215
and Dipartimento di Scienze Fisiche, Mostra D'Oltremare, Pad 19, 80125, Napoli, Italy

Naeem Jan

Department of Physics, Saint Francis Xavier University, Antigonish, Nova Scotia, Canada B2G 1C0

H. Eugene Stanley

Center for Polymer Studies and Department of Physics, Boston University, Boston, Massachusetts 02215
(Received 27 June 1988)

We address the problem of obtaining reliable statistical information on two tricritical points of recent interest, the θ point (conventionally modeled by the self-avoiding walk with nearest-neighbor attractive interactions) and the θ' point (the self-avoiding walk with nearest-neighbor interactions and a subset of the next-nearest-neighbor interactions). Specifically, we show how two very special walk algorithms can provide sufficient statistical information to elucidate fully the multicritical properties. We carry out a Monte Carlo calculation of the exponents at the θ and θ' points using these special walk algorithms. We also examine the crossover behavior along a critical surface that contains both points. Our numerical results suggest that the universality class is changing continuously along this critical surface, so that the θ and θ' points belong to distinct universality classes.

I. INTRODUCTION

The self-avoiding walk (SAW) is known to describe the critical properties of a long linear polymer in a good solvent, where interactions between segments of the polymer are negligible and the excluded volume repulsion is the dominant constraint.[1] As the temperature T is lowered, the attractive interactions between monomers become comparable to kT and as T reaches a special temperature θ, the linear polymer undergoes an abrupt change from the expanded conformation for $T > \theta$ to a fully compact conformation for $T < \theta$. Exactly at $T = \theta$ the chain takes on a well-defined conformation *intermediate* between the conformations above and below θ. The point $T = \theta$ is a tricritical point, termed the θ point.[2]

The properties of such a tricritical point are quantified in the following by three exponents ν, γ, and ϕ.

(i) The correlation length exponent ν is defined by

$$\langle R_N^2 \rangle \sim N^{2\nu} , \tag{1}$$

where $(\langle R_N^2 \rangle)^{1/2}$ is the rms end-to-end distance of a polymer composed of N monomers.

(ii) If we represent the linear polymer by an N-step nonintersecting random walk on a lattice with coordination number q, then we define the enhancement factor exponent γ by

$$C_N \sim \mu^N N^{\gamma - 1} , \tag{2}$$

where C_N is the number of nonintersecting random walks

of N steps, and the connective constant μ plays the role of an *effective* coordination number ($\mu < q - 1$).

(iii) The crossover exponent ϕ is defined by the tricritical-point scaling relation

$$\langle R_N^2 \rangle \sim N^{2\nu} f(\tau N^\phi) , \tag{3}$$

where f is a scaling function and $\tau \equiv (T - \theta)/\theta$.

II. MODELING INTERACTING POLYMERS

We model the polymer conformations near the θ point for dimension $d = 2$ with the configurations of nonintersecting random walks. The relations given in Eqs. (1)–(3) are defined asymptotically as $N \to \infty$. We would therefore like to study the configurational properties of very long walks. However, the number of distinct configurations increases rapidly with N. Because of the quantity of computer time required, exact enumeration algorithms to generate and catalog all configurations by computer have been limited to very short walks (e.g., $N \leq 42$ on the honeycomb lattice[3]). We will therefore employ a Monte Carlo approach, in which we randomly select a representative sample from the set of all walk configurations. As this random subset becomes larger, the statistical error implicit in this method becomes smaller. We will focus on three algorithms, termed SAW, SKW, and KGW (to be defined below); first we discuss (a) straightforward sampling and later we discuss (b) importance sampling.

(a) *Straightforward sampling.* SAW configurations may

be generated by computer with a very simple algorithm which achieves straightforward sampling of configurations from the set of all nonintersecting random walks. One simply launches a random walker on a lattice and, for each successive step, randomly chooses one of the available forward directions. The probability associated with each step is therefore $1/(q-1)$. The probability associated with generating a given configuration, c, of N steps, $P_N^{SAW}(c)$, is the product of these single-step probabilities,

$$P_N^{SAW}(c)=(1/q)\prod_{i=2}^{N}\frac{1}{q-1}=(\tfrac{1}{3})(\tfrac{1}{2})^{N-1} , \qquad (4)$$

where the second equality applies to the honeycomb lattice. The walk is terminated whenever the walker encounters a portion of itself, and thus violates the self-avoiding condition. Since all steps are taken with equal probability, all walks of N steps have the same total probability of being generated, regardless of their particular configuration. This simple algorithm therefore realizes straightforward sampling of nonintersecting random walks since configurations are selected without bias.

We now connect the probability for generating *walk configurations* in the above algorithm with the probability with which *polymer configurations* occur. The probability of observing a polymer chain to have a configuration c is proportional to a Boltzmann factor, $\exp[-E(c)/kT]$, where $E(c)$ is the energy associated with c. We must therefore decide how to assign the energy $E(c)$ to the configuration c. There are two contributions to $E(c)$: (i) The contribution due to excluded volume (the hard-core repulsion of chain segments) requires that a configuration which is not self-avoiding should have an infinite energy, and thus occur with zero probability; this is accounted for by considering *only* self-avoiding configurations; (ii) the contribution due to the effect of *attractive* van der Waals forces between monomers is reflected in the assignment of an energy $J_{NN}<0$ to each nearest-neighbor (NN) contact in the chain and neglecting all longer-range interactions.[4-6] If there are N_{NN} such NN contacts in configuration c, then $E(c)=N_{NN}J_{NN}$. The Boltzmann factor for this configuration is, therefore,

$$\exp[-E(c)/kT]=\exp[-N_{NN}J_{NN}/kT] . \qquad (5)$$

Since the Boltzmann factor in (5) is proportional to the probability of observing a polymer chain in the configuration c, then all configurations would occur with the same probability if $J_{NN}/kT=0$.

The SAW algorithm described above has been used to obtain an ensemble of configurations suitable for modelling linear polymers: The self-avoiding property of the SAW's mimics the excluded volume effect, and the value of N_{NN} for each SAW configuration can be calculated and used to evaluate $E(c)$. In the limit $kT \gg J_{NN}$, or

$$J_{NN}/kT \rightarrow 0 \quad (SAW) , \qquad (6)$$

the ensemble of configurations generated by the SAW algorithm describes the properties of a polymer in a good solvent.[1]

At the θ point, we expect $|J_{NN}|/kT \sim 1$, since this is

the condition needed for the monomer-monomer attractive interactions to be sufficiently significant to approximately balance the effective repulsion due to the excluded volume. Hence, lower-energy configurations with many NN contacts are expected to contribute most to the properties of the θ point. However, the SAW algorithm is found to produce very few configurations with any significant number of NN contacts. The reason is that when such a NN contact occurs, $1/(q-1)$ of the walks terminate due to self-intersection on the next step. As a result, to obtain accurate statistical information for a polymer chain when $T \sim \theta$, enormous numbers of SAW's must be generated. Furthermore, the probability of producing a SAW of length N decreases exponentially with N. Hence enormous numbers of walk "attempts" must be made to obtain a statistically useful set of *long* walks (i.e., $N > 50$). We conclude, therefore, that straightforward sampling of walks with the SAW algorithm is not a very efficient way to simulate θ point polymers.

(b) *Importance sampling.* We would prefer to have a walk generation algorithm which does not suffer from the high attrition rate of the SAW algorithm. We would also like to *preferentially* sample those configurations which have large numbers of NN contacts; that is, we wish to realize "importance sampling." A special type of nonintersecting random walk, called the *smart kinetic walk* (SKW), has exactly these properties.[7,8]

The SKW is a special walk which avoids all self-intersections, with the single exception that the walk may intersect itself at its own origin, to form a ring. Consider, e.g., the honeycomb lattice. The walk is begun by choosing an origin site, and randomly stepping in one of the three directions available (see Fig. 1). We establish the rule that whenever a step is taken in a certain direction, we will place an "X" in the hexagonal cell on the left-hand side of the step, and an "O" in the cell on the right-hand side. The symbol in any cell may not be changed by subsequent steps. Deciding the direction of any given step therefore reduces to randomly choosing an X or O (with equal probability) to fill the cell directly ahead of the previous step. The walk grows such that an X is always on the left and an O is on the right. As the walk continues to grow, it often finds that the cell directly ahead has already been assigned a symbol. In this circumstance no random choice is required; it *must* move in the direction which keeps opposite symbols on either side. We will call such a step a "forced step:" a forced step is taken with a probability p of unity, whereas $p=1/(q-1)=\tfrac{1}{2}$ for an "unforced step" [Fig. 2(a)].
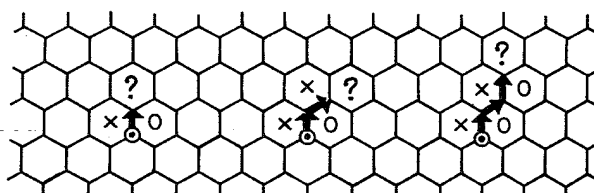

FIG. 1. The first three steps of a typical SKW on the honeycomb lattice. Note how the walker is building a wall of X's on its left, and a wall of O's on its right.
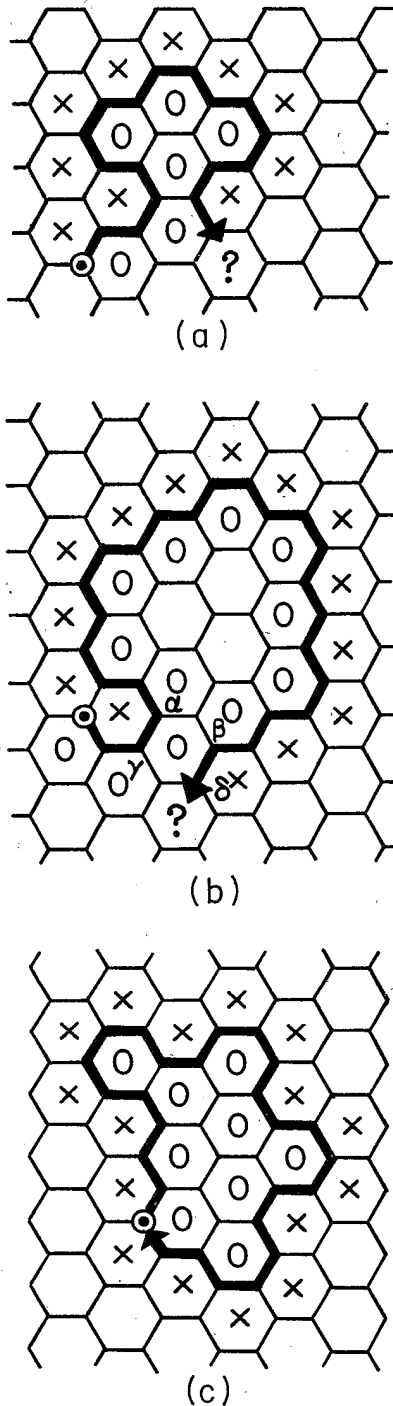
(a)

(b)

(c)

FIG. 2. (a) A forced step in a SKW, taken to avoid self-intersection. The last step shown could not have been taken otherwise, since this would have violated the restriction against moving between two cells of the lattice containing the same symbol. (b) The last step shown here was also "forced," but would not have led to self-intersection if it had been taken otherwise. However, it would have led to the walker entering a "cul de sac," which would have eventually caused termination of the walk. Note that the forced step shown here leaves from a site β which is a NNN of the site α; the subsequent step is not forced and leaves from δ, which is a NNN of γ. Hence, the forced steps taken to avoid cul de sacs are a subset of the NNN contacts. (c) An example of how the SKW algorithm can form a ring without violating any of its rules.

These special rules prevent the walk from ever intersecting itself, since this would require the walker to make a disallowed step through the "protective wall" of X's or O's that surround the walk. These rules also prevent the walker from entering *cul de sacs*—that is, those structures of the walk itself from which the walker could not exit once entered [see Fig. 2(b)]. Thus we have a walk with the strong "survival" characteristic which we desired, and large numbers of walks *with lengths of several thousand steps* may be produced (2 orders of magnitude larger than with straightforward sampling). Note, however, that the rules do not protect against self-intersections at the origin, and in such a case the walk is terminated [see Fig. 2(c)]. Figure 3 shows a typical SKW of 5000 steps, generated in this way.

From Figs. 1 and 2 we see that those forced steps taken to avoid direct self-intersections are in 1:1 correspondence with all NN contacts of the walk with itself. On the other hand, those forced steps taken to avoid *cul de sacs* correspond to a subset of all the next-nearest-neighbor (NNN) contacts which occur in the walk, as shown rigorously in Ref. 9.

To calculate the probability with which SKW configurations are generated we must take into account the details of how the SKW algorithm preferentially generates walks with large numbers of forced steps. Each unforced step is taken with probability $p = \frac{1}{2}$; each forced step is taken with $p = 1$. The total probability $P_N^{\text{SKW}}(c)$ of generating a given SKW configuration of N steps is, therefore,

$$P_N^{\text{SKW}}(c) = (\tfrac{1}{3})(\tfrac{1}{2})^{N-1}(2)^{N_f(c)} , \qquad (7)$$

where $N_f(c)$ is the number of forced steps in the configuration c. Note that $N_f = N_{\text{NN}} + N'_{\text{NNN}}$, where N_{NN} is the number of NN contacts in the SKW, and
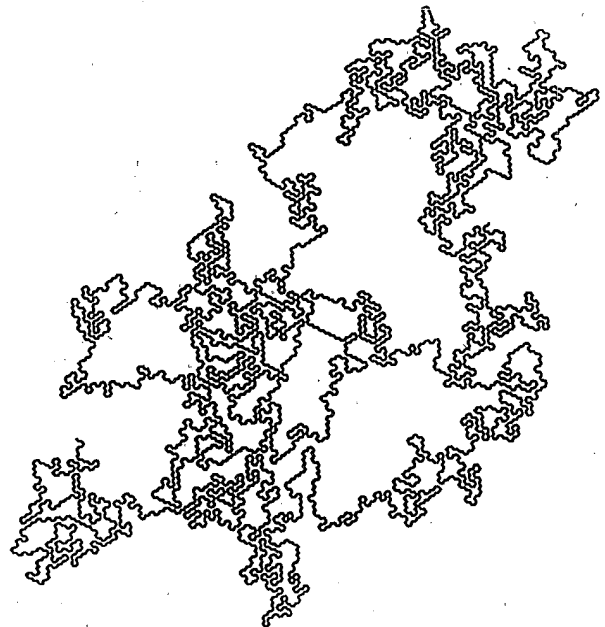

FIG. 3. A typical SKW of 5000 steps, on the honeycomb lattice.

N'_{NNN} is the number of the special subset off NNN contacts. From Eq. (4), (7) becomes

$$P_N^{SKW}(c) = (\tfrac{1}{3})(\tfrac{1}{2})^{N-1} \exp[N_f(c)\ln2] .$$

$$= P_N^{SAW}(c) \exp[N_f(c)\ln2] . \tag{8}$$

We can establish a connection between $P_N^{SKW}(c)$ and the Boltzmann factor for the polymer configuration c, if we assign interaction strengths J_{NN}, for the NN contacts in the polymer chain, and J'_{NNN}, for the special subset of NNN contacts. If we set $J_{NN} = J'_{NNN} = J_f$, then $E(c) = J_f(N_{NN} + N'_{NNN}) = J_f N_f$, and

$$\exp[-E(c)/kT] = \exp(-N_f J_f/kT) . \tag{9}$$

Comparison of (8) and (9) shows that when we define the energy of a polymer chain as above, then the SKW algorithm generates walk configurations with the same relative probability as for polymer configurations when

$$J_f/kT = -\ln2 \quad (\text{SKW}) . \tag{10}$$

Thus for the SKW (10) is the analog of (6) for the SAW. Using the SKW algorithm to generate an ensemble of walks therefore realizes our desired high-efficiency importance sampling of nonintersecting walk configurations: An ensemble of SKW's is generated with the same statistics as an ensemble of nonintersecting random walks with a *nonzero* interaction energy $J_f/kT = -\ln2$.

There is one difficulty with using the SKW algorithm to generate configurations. Since an SKW never enters a *cul de sac*, SKW configurations with either endpoint in such a *cul de sac* are never generated. In other words, an SKW of N steps *always* has the potential to form a ring at some subsequent time. However, the set of all nonintersecting walks of N steps includes such configurations with a trapped endpoint. The set of all SKW's is, therefore, *not* in 1:1 correspondence with the set of all nonintersecting walks because the SKW algorithm excludes the possibility of generating walks with endpoints in *cul de sacs*. For this reason, it is not possible to calculate certain of the properties defined in Eqs. (1)–(3) from an ensemble of SKW's.

There exists another special type of walk which does not suffer from the above defect, known as the kinetic growth walk (KGW).[10] This walk is an extension of the SAW algorithm discussed above. To make a KGW, the random walker "looks ahead" one step as it walks, and chooses randomly from only unoccupied NN sites for the destination of its next step. In this way, direct self-intersection, including ring formation, is avoided, but trapping in *cul de sacs* occurs. Hence, the KGW configurations are in 1:1 correspondence with the set of all nonintersecting walks. However, since the KGW suffers from attrition due to trapping in *cul de sacs* the KGW algorithm is not as efficient as the SKW algorithm in producing long walks; typically, meaningful numbers of KGW's up to only a few hundred steps may be generated in two dimensions.

We can calculate the probability with which an N step KGW is generated. On the honeycomb lattice we find that

$$P_N^{KGW}(c) = (\tfrac{1}{3})(\tfrac{1}{2})^{N-1}(2)^{N_{NN}(c)}$$

$$= P_N^{SAW}(c) \exp[N_{NN}(c)\ln2] , \tag{11}$$

where $N_{NN}(c)$ is the number of forced steps taken to avoid direct self-intersection, and which therefore correspond to NN contacts.

To relate P_N^{KGW} to the Boltzmann factor for the polymer configuration c, we assign an interaction strength J_{NN} to each of the NN contacts in c. Hence $E(c) = J_{NN} N_{NN}$ and

$$\exp[-E(c)/kT] = \exp[-N_{NN} J_{NN}/kT] . \tag{12}$$

This means that the KGW algorithm generates walk configurations with the same relative probability as for polymer configurations when

$$J_{NN}/kT = -\ln2 \quad (\text{KGW}) . \tag{13}$$

For the KGW (13) is the analog of (10) and (6). Thus the KGW algorithm also realizes importance sampling of nonintersecting walks, albeit less efficiently than does the SKW. An ensemble of KGW's are generated with the same statistics as an ensemble of nonintersecting random walks having an interaction energy of $J_{NN}/kT = -\ln2$.

Our discussion is summarized in Fig. 4 and Table I. Figure 4(a) shows a phase diagram with three points indicating where each of the above algorithms generates the correct ensemble. Figure 4(b) shows the relative efficiency of each algorithm in producing long walks on the honeycomb lattice.

III. TRICRITICAL EXPONENTS

The θ point is conventionally modelled with nonintersecting random walks in which only NN interactions of strength J_{NN} contribute to the energy of the chain. However, the exact value of the critical NN interaction energy $J_{NN}/k\theta$ is not known; neither are there exact values for the critical exponents which characterize the properties of the NN interacting chain at $T = \theta$ except above the critical dimension $d_c = 3$.

Given the efficiency of the SKW in generating long walks, it would seem reasonable to model θ-point configurations with SKW's. We have shown that the SKW algorithm generates an ensemble of configurations weighted according to NN *and* a special subset of NNN contacts, such that $J_f/kT = -\ln2$. The SKW algorithm does not generate the full set of nonintersecting walks, but it has been shown by Duplantier and Saleur[11] (DS) that if each member of the full set of SAW's (which *is* in 1:1 correspondence with all nonintersecting walks) is weighted by exactly

$$\exp[-(N_{NN} + N'_{NNN})J_f/kT] = \exp(N_f \ln2) ,$$

then the resulting ensemble possesses critical exponents which put it in a different universality class from that of the dilute $(T \to \infty)$ or collapsed $(T \to 0)$ polymer chain. This critical interaction energy $J_f/KT = -\ln2$ therefore defines a higher-order critical point which has been called the θ' point,[9] to distinguish it from the θ point where only NN interactions are considered.
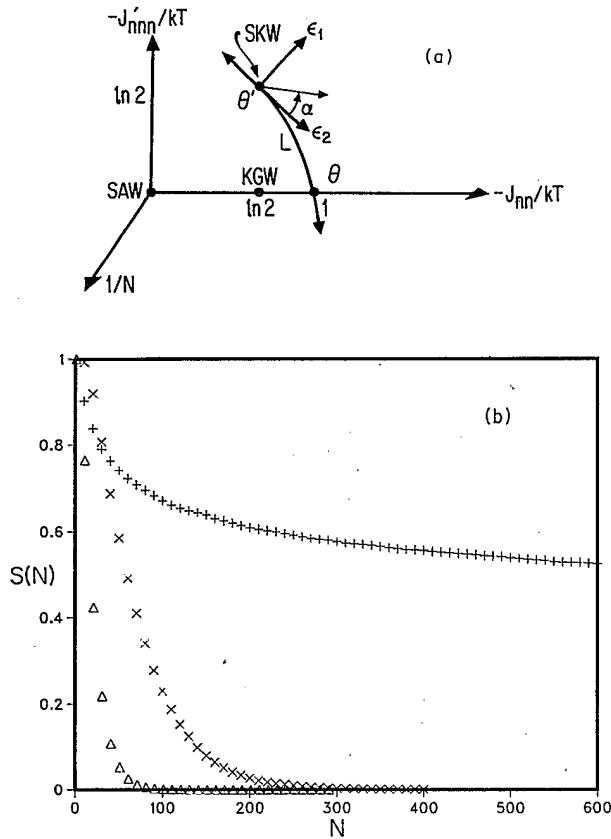
FIG. 4. (a) Phase diagram for the two systems treated in this paper, the θ' point and the θ point. The critical value $|\epsilon_c|$ of the interaction parameter $|\epsilon| \equiv |J_{NN}|/kT$ of the θ point is near unity, based on calculations reported in the text and Fig. 6. Also located are the points where the three special walk algorithms described in the text generate the correct ensemble of configurations; note that the point of the SKW algorithm coincides with the θ' point. The line L labels a critical surface which includes both the θ and θ' points; ϵ_1 and ϵ_2 label the two relevant scaling field axes at the θ' point—one tangential to L and one perpendicular. (b) A plot of $S(N)$, the probability that a walk has not terminated by its Nth step, vs N, for the SKW ($+$), KGW ($\times$), and SAW ($\triangle$) algorithms.

In this paper, we address the question of whether the θ and θ' points possibly belong to the same universality class. This question is of particular recent interest because DS have found exact expressions for $d=2$ for the three tricritical exponents of the θ' point. If the θ and θ' points were in the same universality class, then the DS results would apply to the θ point as well, and hence would be directly relevant to experiments on quasi-two-dimensional polymers.[12] DS proposed that the θ and θ' points do indeed belong to the same universality class, but their proposal has been questioned[13-15] because the NNN interaction is of a very special sort and because of results[16] on the analogous *branched* polymer problem.

First we calculate for each point the three tricritical exponents ν, γ, and ϕ defined in Eqs. (1)–(3). DS have argued that the exact values of the tricritical exponents at the θ' point are[17] $\nu_{\theta'} = \frac{4}{7}$, $\gamma_{\theta'} = \frac{8}{7}$, and $\phi_{\theta'} = \frac{3}{7}$. In order to test these predictions, and to make a comparison to the θ point, we exploit the special nonintersecting walk algorithms described earlier.

A. The θ' point

At the θ' point, the SKW is clearly the best model since it efficiently produces configurations with exactly the correct weights for the θ' point. However, the SKW algorithm does not generate configurations with endpoints in *cul de sacs*, raising the question of which critical exponents can be calculated from an ensemble of SKW's. Since it is not clear how the number of SKW's of N steps is related to C_N, we cannot find γ from a SKW ensemble. We will show, however, that it is possible to find ν and ϕ for the set of all nonintersecting walks from an ensemble of SKW's.[9]

Consider the fractal dimension $d_f = 1/\nu$. If we take a section from a very long walk which is far from either end of the walk, then this middle section will necessarily not have its ends within *cul de sacs*. Due to the self-similarity of nonintersecting random walks,[18] this middle section will have the same fractal dimension as the entire walk from which it was extracted. Therefore, the subset

TABLE I. A comparison of the three algorithms described in the text for generating self-avoiding configurations. The first line indicates the location in the phase diagram of Fig. 4(a) where each algorithm generates the correct ensemble of configurations for modelling interacting polymers.

	SAW	KGW	SKW
Interaction [cf. Fig. 4(a)]	$J_{NN}/kT = 0$	$J_{NN}/kT = -\ln 2$	$J_{NN}/kT = J'_{NNN}/kT = -\ln 2$
Typical maximum walk length	100	1000	10 000
Attrition mechanisms	Direct self-intersection Trapping in *cul de sacs*	Trapping in *cul de sacs*	Direct self-intersection at origin (ring formation)
Comparison with SAW		All SAW configurations present	Some SAW configurations missing

of nonintersecting walks produced by the SKW algorithm, which do not have endpoints in *cul de sacs*, may be used to calculate the exponent ν for the full set of nonintersecting walks. The above considerations apply for any value of τ, and so the exponent ϕ may be found from an ensemble of SKW's.

(a) To find $\nu_{\theta'}$ using the SKW algorithm, we calculate $\langle R_N^2 \rangle$ for a large number of SKW's and make a log-log plot of $\langle R_N^2 \rangle$ versus N, shown in Fig. 5(a). The asymptotic slope gives $2\nu_{\theta'}$; we find $\nu_{\theta'}=0.57\pm0.01$.

(b) To find $\phi_{\theta'}$, we note from (3) that for both the θ and θ' points

$$Q_N \equiv \frac{1}{\langle R_N^2 \rangle} \left[\frac{\partial \langle R_N^2 \rangle}{\partial \tau} \right]_{\tau=0} \sim N^\phi . \tag{14a}$$

Since

$$\langle R_N^2 \rangle \equiv \frac{\sum_c R_N^2(c) \exp[-E(c)/kT]}{\sum_c \exp[-E(c)/kT]} , \tag{14b}$$

we can form the derivative in (14a) and so express Q_N in terms of quantities that may be calculated. In terms of calculated quantities, (14a) takes the form

$$Q_N \propto \frac{\langle N_f R_N^2 \rangle - \langle N_f \rangle \langle R_N^2 \rangle}{\langle R_N^2 \rangle} . \tag{15}$$

Figure 5(b) shows a log-log plot of Q_N against N; the asymptotic slope gives $\phi_{\theta'}=0.45\pm0.03$.

(c) In order to find $\gamma_{\theta'}$ we must ensure that the set of all nonintersecting walks is sampled, and so we use the KGW algorithm. The KGW algorithm generates chains with the statistics of an ensemble of walks with NN interaction $J_{NN}/kT=-\ln2$. To obtain θ' point statistics, for which the interaction is $J_f/kT=-\ln2$, we must adjust the weight of each KGW: the proper weight

$$P_N^{\theta'}(c) = P_N^{SKW}(c) \tag{16a}$$

for each KGW configuration at the θ' point is produced by weighting each KGW configuration explicitly by $\exp(N'_{NNN}\ln2)$. That is, from a comparison of (8) and (11),

$$P_N^{\theta'}(c) = P_N^{KGW}(c) \exp(N'_{NNN}\ln2)$$

$$= P_N^{SAW}(c) \exp[(N_{NN}+N'_{NNN})\ln2] . \tag{16b}$$

The result is a KGW-generated ensemble of all weighted SAW's.

To measure $\gamma_{\theta'}$, we consider the survival probability $S(N)$, the probability that a given walk will survive to N steps:

$$S(N) \equiv \frac{C_N}{C_N^{RW}} \sim \left[\frac{\mu}{z} \right]^N N^{\gamma-1} . \tag{17}$$

$C_N^{RW}=z^N$ is the number of random walks of N steps, and $z=q-1$. We can therefore write[19]

$$\ln\left[\frac{S(N+12)}{S(N-12)} \right] \sim 24\ln\left[\frac{\mu}{z} \right] + (\gamma-1)\ln\left[\frac{N+12}{N-12} \right] . \tag{18}$$
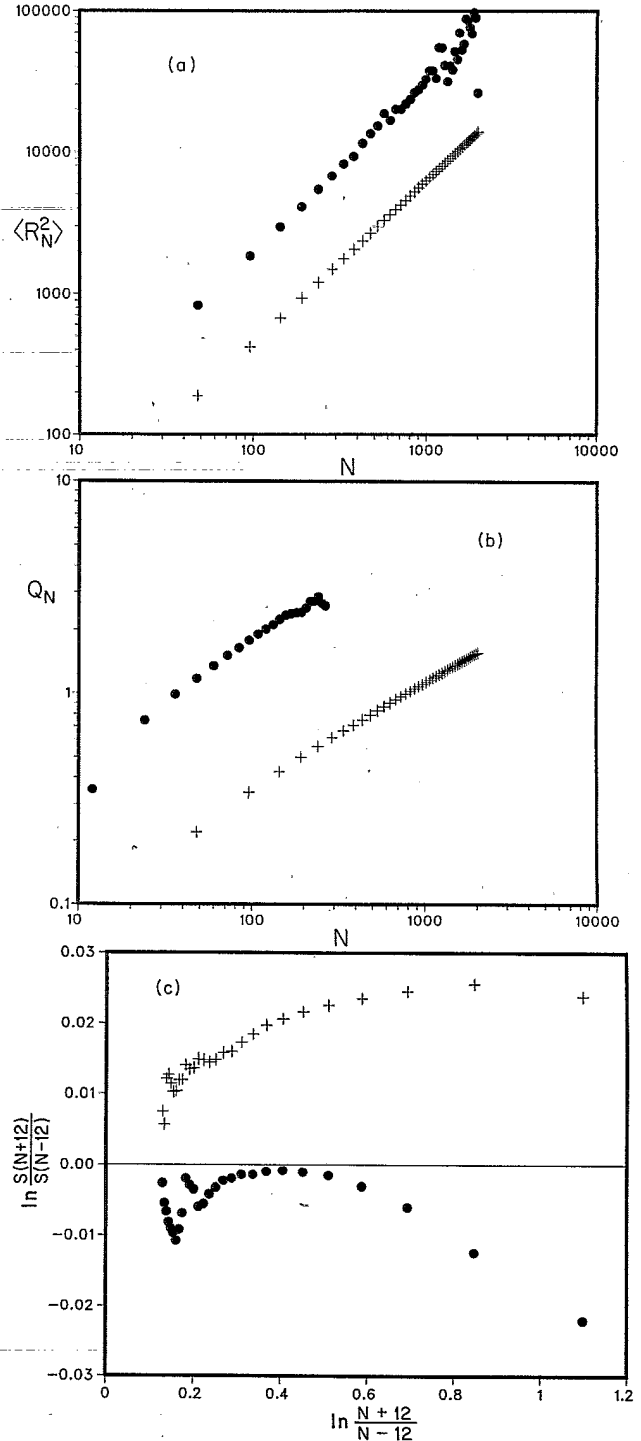

FIG. 5. (a) A log-log plot of $\langle R_N^2 \rangle$ vs N for the θ point (●) and θ' point ($+$); the θ point values have been doubled in order to separate the curves on the same plot. The asymptotic slopes give $2\nu_\theta$ and $2\nu_{\theta'}$. (b) A log-log plot of Q_N [as defined in Eq. (14a)] against N for the θ (●) and θ' ($+$) points; the θ' point values have been multiplied by $\frac{1}{2}$ to separate the curves. The θ point curve becomes prohibitively "noisy" for $N>300$, and is not extended further here. The asymptotic slopes give ϕ_θ and $\phi_{\theta'}$. (c) A plot of $\ln[S(N+12)/S(N-12)]$ vs $\ln[(N+12)/(N-12)]$ for the θ (●) and θ' ($+$) points; for purposes of comparison, the θ point values have been altered by an additive constant of -0.8. The limiting slopes as $N\rightarrow\infty$ give $\gamma_\theta-1$ and $\gamma_{\theta'}-1$.

The number 12 is chosen to minimize lattice oscillations. The asymptotic slope of a log-log plot of $S(N+12)/S(N-12)$ versus $(N+12)/(N-12)$ has slope $\gamma_{\theta'}-1$. With this approach we find $\gamma_{\theta'}=1.12\pm0.07$ [see Fig. 5(c)].

B. The θ point

To evaluate the exponents at the θ point, we must first find the critical value $J_{NN}/k\theta$. We use the KGW since only NN interactions are used to model the θ point. By weighting each KGW configuration with a more general Boltzmann factor $\exp[-(\epsilon+\ln2)N_{NN}]$, where $\epsilon=J_{NN}/kT$, we obtain a general weight $P_N(c)$ given by

$$P_N(c)=P_N^{KGW}\exp[-(\epsilon+\ln2)N_{NN}]$$
$$=P_N^{SAW}\exp(-\epsilon N_{NN}) , \qquad (19a)$$

which makes it possible to explore all temperatures along the J_{NN}/kT axis in Fig. 4(a). (See however, the Appendix.) Numerical results indicate that this weighted KGW ensemble describes a tricritical point when $\epsilon+\ln2 =\epsilon_c+\ln2=-0.30\pm0.05$, so that $J_{NN}/k\theta=\epsilon_c =-0.99\pm0.05$ (see Fig. 6). This is the conventional θ-point.

Having found ϵ_c, we can adjust the weight of both KGW's and SKW's to obtain θ-point statistics. In analogy with (16b), the proper weight $P_N^\theta(c)$ for a configuration c at the θ point can be expressed in terms of $P_N^{KGW}(c)$ and $P_N^{SKW}(c)$. From (19a), with $\epsilon=\epsilon_c$, we have

$$P_N^\theta(c)=P_N^{SAW}\exp(-\epsilon_c N_{NN}) . \qquad (19b)$$
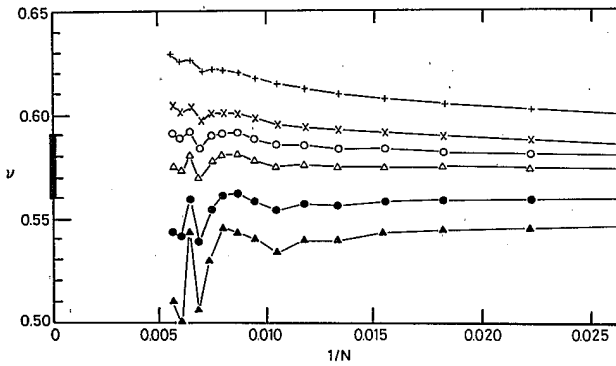
Using (11) in (19b), the proper weight for each KGW at

the θ point is

$$P_N^\theta(c)=P_N^{KGW}\exp[-(\epsilon_c+\ln2)N_{NN}] . \qquad (19c)$$

Using (8) in (19b), the proper weight for each SKW at the θ point is

$$P_N^\theta(c)=P_N^{SKW}\exp[-\epsilon_c N_{NN}-(\ln2)N_f]$$
$$=P_N^{SKW}\exp[-(\epsilon_c+\ln2)N_{NN}-(\ln2)N'_{NNN}] , \qquad (19d)$$

since $N_f=N_{NN}+N'_{NNN}$. With the same analysis as at the θ' point, we use an ensemble of SKW's weighted as in (19d) to find $\nu_\theta=0.60\pm0.05$ and $\phi_\theta=0.5\pm0.1$ [see Figs. 5(a) and 5(b)]. Using an ensemble of KGW's weighted as in (19c), we find $\gamma_\theta=1.08\pm0.07$ [see Fig. 5(c)].

The above numerical results therefore confirm the DS prediction for the tricritical exponents at the θ' point. Although our values for the θ-point exponents are consistent with the corresponding θ'-point values within the confidence limits of our calculation, it is difficult to conclude from this work whether the θ and θ' points belong to the same universality class. Hence, in the next section we investigate more closely the properties of the θ' point, where configurations may be generated with great efficiency with the SKW algorithm.

IV. CROSSOVER BEHAVIOR NEAR THE θ' POINT

In the phase diagram shown in Fig. 4(a), we expect a critical line L to connect the θ and θ' points. If the θ' point is a critical point of higher order with respect to the rest of the line L, we expect another crossover exponent $\phi_2>0$ in a special direction tangent to L at θ'. To demonstrate this, we establish two orthogonal scaling field axes, ϵ_1 and ϵ_2, such that ϵ_2 is tangent to L at θ'. The scaling relation of Eq. (3) therefore generalizes[20] to

$$\langle R_N^2 \rangle \sim N^{2\nu_{\theta'}}f(\epsilon_1 N^{\phi_1},\epsilon_2 N^{\phi_2}) . \qquad (20)$$

The exponent ϕ_1 determines the crossover behavior near θ' with respect to the collapsed and dilute regimes on either side of L; hence $\phi_1=\phi_{\theta'}$. The exponent ϕ_2 controls how the crossover occurs from the tricritical points on L near θ', to the θ' point itself. If the θ' point is in a *different* universality class from its neighboring tricritical points, then we should measure $\phi_2>0$; in the language of renormalization group, this means that the scaling field ϵ_2 is a relevant parameter. On the other hand, if the θ' point belongs to the *same* universality class as the rest of the line L, then we will find $\phi_2<0$, and ϵ_2 will be an irrelevant parameter. The marginal case $\phi_2=0$ corresponds to the more complex situation in which the critical exponents may vary continuously along the critical line.

By the same argument leading to Eq. (14a), we find that

$$Q_\alpha \equiv \frac{1}{\langle R_N^2 \rangle}\left[\frac{\partial\langle R_N^2\rangle}{\partial\epsilon_\alpha}\right]_{\epsilon_1=\epsilon_2=0}$$
$$\sim A(\alpha)N^{\phi_1}+B(\alpha)N^{\phi_2} . \qquad (21)$$

The above derivative is a directional one taken along a line ϵ_α at an angle α with respect to the ϵ_2 axis, so that ϵ_α

FIG. 6. Analysis of the weighted KGW near the θ point for several values of the interaction parameter $\epsilon+\ln2$: -0.200 ($+$); -0.250 ($\times$); -0.275 ($\circ$); -0.300 ($\triangle$); -0.350 ($\bullet$); and -0.400 ($\blacktriangle$). For finite N we define an effective exponent $\nu(N)=\frac{1}{2}\ln[\langle R^2(N+1)\rangle/\langle R^2(N)\rangle]/\ln[(N+1)/N]$, where $R(N)$ is the radius of gyration of a chain of length N. The extrapolation of $\nu(N)$ to $N\to\infty$ determines ν. This analysis is usually reserved for series expansions, but high-quality Monte Carlo data may also be analyzed in this manner. We find that for $T>\theta(\epsilon>\epsilon_c)$, $\nu(N)$ increases with N and extrapolates toward the SAW value, while for $T<\theta(\epsilon<\epsilon_c)$, $\nu(N)$ extrapolates to the collapsed phase. At $T=\theta$ ($\epsilon_c+\ln2=-0.300$) we find that $\nu(N)$ extrapolates to a new value, intermediate between these extremes.

is a line such that $\epsilon_1 \cos\alpha = \epsilon_2 \sin\alpha$. The coefficients A and B are functions of α such that when $\alpha = 0$, $A = 0$, and when $\alpha = \pi/2$, $B = 0$. Since we do not know the exact orientation of the ϵ_2 axis with respect to the phase diagram axes in Fig. 4(a), we rewrite Eq. (21) as

$$\frac{Q_\alpha}{N^{\phi_1}} \sim A(\alpha) + B(\alpha)N^{\phi_2 - \phi_1} . \tag{22}$$

If we plot Q_α/N^{ϕ_1} against $1/N^{\phi_1}$ using the predicted value $\phi_1 = \frac{3}{7}$, then the asymptotic N dependence of the curve for any α will be entirely due to the value of ϕ_2. In Fig. 7(a) we form such a plot; the fact that the curves appear asymptotically straight suggests that $\phi_2 \simeq 0$, the marginal case. To measure ϕ_2 explicitly, we obtain the value of $\alpha = \alpha'$ from Fig. 7(a) for which the intercept $A(\alpha) = 0$, and make a log-log plot of $Q_{\alpha=\alpha'}$ versus N [Fig. 7(b)]. The asymptotic slope gives $\phi_2 = 0.0 \pm 0.05$. Our results therefore suggest that the actual situation may in fact be that of the marginal case, where the universality class changes continuously along L.
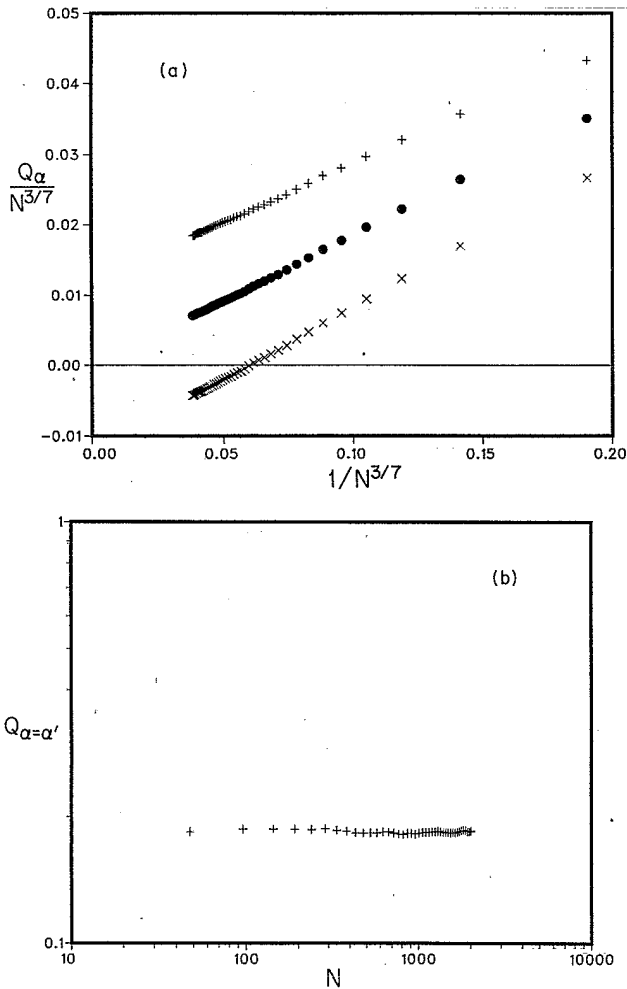
V. DISCUSSION AND CONCLUSIONS

In summary, we have addressed the question of the universality class of the θ and θ' points. We have made an extensive Monte Carlo simulation program for studying both the conventional model of the θ point and the model which displays a tricritical point called a θ' point. We present numerical evaluations of the tricritical exponents at both points. These values confirm the DS predictions for the θ' point, and indicate an upper limit on how different the exponents at each point can be. Finally, our examination of the crossover behavior at the θ' point suggests that the universality class varies in a complex manner along the line that contains the θ and θ' points, supporting the possibility that they do not belong to the same universality class. We conclude by noting that for dimension $d > 2$, it has been shown[21,22] that the θ and θ' points *are* in the same universality class. However, the methods of this proof do not extend to $d \leq 2$. Since our work is in $d = 2$, our suggestion that the θ and θ' points are not in the same universality class is not inconsistent with the above proof.

FIG. 7. (a) Plot of $Q_\alpha/N^{3/7}$ vs $1/N^{3/7}$ for three values of tangent angle α: $\alpha = 54°$ ($+$), $\alpha = 57°$ ($\bullet$), and $\alpha = 60°$ ($\times$). The straightness of these curves suggests $\phi_2 \simeq 0$. (b) Log-log plot of $Q_{\alpha=\alpha'}$ against N. The asymptotic slope gives ϕ_2.

APPENDIX: COMMENT ON STATISTICAL ERRORS

The following remarks concern the estimates for ν_θ, ϕ_θ, γ_θ, and $\gamma_{\theta'}$, given in Sec. III. We first discuss the KGW algorithm. This algorithm can generate any configuration of nonintersecting random walk, but as we have noted, not all KGW configurations are generated with equal probability. Note that the probability $P_N^{KGW}(c)$ in (11) is a function of only N_{NN}, and hence the probability $P_N^{KGW}(N_{NN})$ to generate a KGW with N_{NN} NN contacts coincides with the more general probability $P_N(N_{NN})$ in (19a) to observe a polymer chain with N_{NN} NN contacts when $\epsilon = -\ln 2$.

For the polymer system, the probability $P_N(E)$ to observe a polymer in a configuration of energy E can be written as

$$P_N(E) = \Omega_N(E) \exp(-\beta E) , \tag{A1}$$

where $\Omega_N(E)$ is the degeneracy of N step configurations having energy E, and $\beta \equiv 1/kT$. In general, $P_N(E)$ is expected to be a sharply peaked function of E because it is the product of a rapidly *increasing* function of E, $\Omega_N(E)$, and a rapidly *decreasing* function of E, $\exp(-\beta E)$.

Since $E = J_{NN} N_{NN}$, (19a) implies

$$P_N(E/J_{NN}) = P_N(N_{NN})$$

$$= P_N^{KGW}(N_{NN})\exp[-(\epsilon + \ln2)N_{NN}] . \quad (A2)$$

The behavior of $P_N(E)$ can therefore be calculated directly from knowledge of $P_N^{KGW}(N_{NN})$. Now $P_N^{KGW}(N_{NN})$ can be estimated with the KGW algorithm, by making a histogram showing the number of walks generated having N_{NN} NN contacts, and normalizing by the number of walks in the sample. For example, the left curve of Fig. 8 shows $P_N^{KGW}(N_{NN})$ for KGW's of length $N = 200$. The relatively narrow shape of this curve implies that the most probable configurations are confined to a well-defined interval of N_{NN}; these contribute most to the statistics of chains at $\epsilon = -\ln2$.

Now consider the case $\epsilon \neq -\ln2$. We require a set of configurations weighted according to $P_N(N_{NN})$ of (A2). Substituting the result for $P_N^{KGW}(N_{NN})$ from the *left* curve of Fig. 8 into (A2), $P_N(N_{NN})$ can be easily calculated. The result for $\epsilon = -0.9 < -\ln2$ is shown as the *right* curve in Fig. 8. The peak has shifted, reflecting the fact that at a lower temperature the most probable configurations have more NN contacts.

Note that the right curve has greater scatter than the left curve. The explanation of this effect is quite revealing. Consider, e.g., $N_{NN} = 40$, which corresponds to the peak of the right curve. The KGW configurations that produce the right curve are very few in number, since $N_{NN} = 40$ is in the tail of the original distribution. *Thus a relatively small fraction of the left curve is used to obtain much of the right curve.* Thus we see that the right curve has little statistical error for *small* values of N_{NN} but larger statistical error for *large* values of N_{NN}.

In general, the fraction of the Monte Carlo sample that makes a meaningful contribution to the chain statistics for a given value of ϵ *decreases* as $|\epsilon - \ln2|$ *increases*. The rate of decrease depends both on how fast the peak of $P_N(N_{NN})$ moves away from the peak of $P_N^{KGW}(N_{NN})$ as $|\epsilon - \ln2|$ increases, and on how quickly the tails of $P_N^{KGW}(N_{NN})$ decrease with respect to N_{NN}.

The result is an effective reduction in sample size when KGW's are weighted as in (A2) to give θ point statistics. A completely analogous effective reduction in sample size occurs when KGW's are weighted as in (16b) to give θ' point statistics. This contributes to the scatter observed in both curves of Fig. 5(c), and hence to the uncertainty
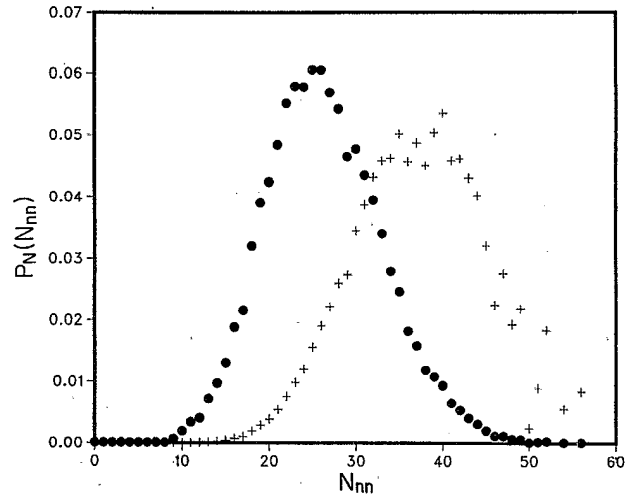

FIG. 8. A plot of $P_N(N_{NN})$ vs N_{NN} for a sample of KGW's of length $N = 200$, for $\epsilon = -\ln2$ (●) and $\epsilon = -0.9$ (+).

in the values for γ_θ and $\gamma_{\theta'}$.

Weighting SKW's as in (19d) also results in the effective reduction of the sample size. Hence the curve in Fig. 5(a) giving ν_θ and the curve in Fig. 5(b) giving ϕ_θ are much noisier than the corresponding θ' point curves.

This effective reduction in the sample size places a limit upon how large $|\epsilon - \ln2|$ can be. The numerical estimate for $P_N^{KGW}(N_{NN})$ cannot extend beyond values of N_{NN} for which configurations are obtained. Hence, there must be values of ϵ for which chain statistics can not possibly be studied with the KGW algorithm because *none* of the dominant chain configurations for those values of ϵ are generated. In general, one can expect to explore a range of ϵ for which clearly peaked $P_N(N_{NN})$ distributions can be formed from the $P_N^{KGW}(N_{NN})$ curve. A limitation of the present work is that ϵ_c for the θ point seems to lie outside this range, and so considerable scatter is observed in some of the data. Indeed, for $\epsilon_c = -1.0$, our sample size is *effectively* reduced to less than 1% of the original set (generated for $\epsilon = -\ln2$).

We conclude by noting that the above remarks do not concern the estimates for $\nu_{\theta'}$ and $\phi_{\theta'}$ since the required ensemble of configurations in this case is exactly that generated by the SKW algorithm. For the same reason, the results of Sec. IV are unaffected by the above considerations on statistical error.

[1]P. G. de Gennes, *Scaling Concepts in Polymer Physics* (Cornell University Press, Ithaca, 1979). See also the more recent books, M. Doi and S. F. Edwards, *The Theory of Polymer Dynamics* (Oxford University Press, London, 1986); K. F. Freed, *Renormalization Group Theory of Macromolecules* (Wiley, New York, 1987); *Random Fluctuations and Pattern Growth: Experiments and Models,* edited by H. E. Stanley and N. Ostrowsky (Kluwer Academic, Dordrecht, 1988).

[2]P. G. De Gennes, J. Phys. (Paris) Lett. **36**, L55 (1975).

[3]D. MacDonald, D. L. Hunter, K. Kelly, and N. Jan, J. Phys. A (to be published).

[4]A. Baumgartner, J. Phys. (Paris) **43**, 1407 (1982).

[5]K. Kremer, A. Baumgartner, and K. Binder, J. Phys. A **15**, 2879 (1982).

[6]F. Seno and A. L. Stella, J. Phys. (Paris) **49**, 739 (1988).

[7]A. Weinrib and S. A. Trugman, Phys. Rev. B **31**, 2993 (1985).

[8]K. Kremer and J. W. Lyklema, Phys. Rev. Lett. **54**, 267 (1985).

[9]A. Coniglio, N. Jan, I. Majid, and H. E. Stanley, Phys. Rev. B

35, 3617 (1987).

[10]I. Majid, N. Jan, A. Coniglio, and H. E. Stanley, Phys. Rev. Lett. **52**, 1257 (1984).

[11]B. Duplantier and H. Saleur, Phys. Rev. Lett. **59**, 539 (1987). These authors assume that the θ' and θ points are in the same universality class.

[12]R. Vilanove and F. Rondelez, Phys. Rev. Lett. **45**, 1502 (1980).

[13]P. H. Poole, A. Coniglio, N. Jan, and H. E. Stanley, Phys. Rev. Let. **60**, 1203 (1988).

[14]F. Seno, A. L. Stella, and C. Vanderzande, Phys. Rev. Lett. **61**, 1520 (1988).

[15]B. Duplantier and H. Saleur, Phys. Rev. Lett. **61**, 1521 (1988).

[16]A. Coniglio, J. Phys. A **16**, L187 (1983).

[17]It is interesting to note that the result $\nu_{\theta'} = \frac{4}{7}$ follows from the fact that the SKW describes also the critical properties of the incipient infinite cluster in percolation. Hence, $d_{\theta'} = 1/\nu_{\theta'}$—the fractal dimension of a polymer chain at the θ' point—coincides with the exactly known fractal dimension of a percolation hull $d_h = \frac{7}{4}$. See R. M. Ziff, Phys. Rev. Lett. **56**, 545 (1986); H. Saleur and B. Duplantier, *ibid.* **58**, 2325 (1987).

[18]S. Havlin and D. Ben-Avraham, Phys. Rev. A **26**, 1728 (1982).

[19]J. W. Lyklema and K. Kremer, J. Phys. A **17**, L691 (1984).

[20]C. Domb and J. L. Lebowitz, *Phase Transitions and Critical Phenomena*, (Academic, New York, 1984), Vol. 9.

[21]B. Duplantier and H. Saleur, Phys. Rev. Lett. **60**, 1204 (1988).

[22]B. Duplantier, Phys. Rev. A **38**, 3647 (1988).